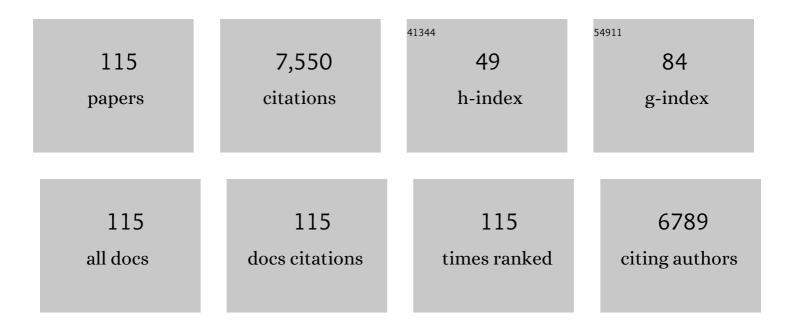
## Ravi K Kukkadapu

List of Publications by Year in descending order

Source: https://exaly.com/author-pdf/2280963/publications.pdf Version: 2024-02-01



ΡΑΛΊ Κ ΚΙΙΚΚΑΠΑΘΙΙ

#	Article	IF	CITATIONS
1	Fast redox switches lead to rapid transformation of goethite in humid tropical soils: A Mössbauer spectroscopy study. Soil Science Society of America Journal, 2022, 86, 264-274.	2.2	4
2	SSSAJ 2021 Publisher's Report. Soil Science Society of America Journal, 2022, 86, 868-878.	2.2	0
3	Susceptibility of new soil organic carbon to mineralization during dry-wet cycling in soils from contrasting ends of a precipitation gradient. Soil Biology and Biochemistry, 2022, 169, 108681.	8.8	11
4	Elemental iron: reduction of pertechnetate in the presence of silica and periodicity of precipitated nano-structures. Environmental Science: Nano, 2021, 8, 97-109.	4.3	2
5	Characterizing the localization of organic C on mineral surfaces: a correlative microscopy/spectroscopy approach. Microscopy and Microanalysis, 2021, 27, 306-307.	0.4	0
6	Lignin-enhanced reduction of structural Fe(III) in nontronite: Dual roles of lignin as electron shuttle and donor. Geochimica Et Cosmochimica Acta, 2021, 307, 1-21.	3.9	27
7	Strong Purcell enhancement at telecom wavelengths afforded by spinel Fe3O4 nanocrystals with size-tunable plasmonic properties. Nanoscale Horizons, 2021, , .	8.0	2
8	Spontaneous redox continuum reveals sequestered technetium clusters and retarded mineral transformation of iron. Communications Chemistry, 2020, 3, .	4.5	8
9	Waterâ€dispersible nanocolloids and higher temperatures promote the release of carbon from riparian soil. Vadose Zone Journal, 2020, 19, e20077.	2.2	2
10	Macro to Nanoscale Approaches to Study Mineral Transformations at the Liquid, Organic, Biological Interface Microscopy and Microanalysis, 2020, 26, 1568-1569.	0.4	0
11	Changes in Sedimentary Phosphorus Burial Following Artificial Eutrophication of Lake 227, Experimental Lakes Area, Ontario, Canada. Journal of Geophysical Research G: Biogeosciences, 2020, 125, e2020JG005713.	3.0	23
12	Role of clay-associated humic substances in catalyzing bioreduction of structural Fe(III) in nontronite by Shewanella putrefaciens CN32. Science of the Total Environment, 2020, 741, 140213.	8.0	19
13	Strong mineralogic control of soil organic matter composition in response to nutrient addition across diverse grassland sites. Science of the Total Environment, 2020, 736, 137839.	8.0	29
14	Calcareous organic matter coatings sequester siderophores in alkaline soils. Science of the Total Environment, 2020, 724, 138250.	8.0	14
15	Dispersible Colloid Facilitated Release of Organic Carbon From Two Contrasting Riparian Sediments. Frontiers in Water, 2020, 2, .	2.3	3
16	Root-driven weathering impacts on mineral-organic associations in deep soils over pedogenic time scales. Geochimica Et Cosmochimica Acta, 2019, 263, 68-84.	3.9	29
17	Electron transfer between sorbed Fe(II) and structural Fe(III) in smectites and its effect on nitrate-dependent iron oxidation by Pseudogulbenkiania sp. strain 2002. Geochimica Et Cosmochimica Acta, 2019, 265, 132-147.	3.9	23
18	Identifying sources and cycling of phosphorus in the sediment of a shallow freshwater lake in China using phosphate oxygen isotopes. Science of the Total Environment, 2019, 676, 823-833.	8.0	34

#	Article	IF	CITATIONS
19	"Switching on―iron in clay minerals. Environmental Science: Nano, 2019, 6, 1704-1715.	4.3	21
20	Uranium storage mechanisms in wet-dry redox cycled sediments. Water Research, 2019, 152, 251-263.	11.3	32
21	Synthesis of nanometer-sized fayalite and magnesium-iron(II) mixture olivines. Journal of Colloid and Interface Science, 2018, 515, 129-138.	9.4	19
22	Iron and Arsenic Speciation During As(III) Oxidation by Manganese Oxides in the Presence of Fe(II): Molecular-Level Characterization Using XAFS, Mössbauer, and TEM Analysis. ACS Earth and Space Chemistry, 2018, 2, 256-268.	2.7	32
23	Physical and electrical properties of melt-spun Fe-Si (3–8 wt.%) soft magnetic ribbons. Materials Characterization, 2018, 136, 212-220.	4.4	20
24	Catalytic N2O decomposition and reduction by NH3 over Fe/Beta and Fe/SSZ-13 catalysts. Journal of Catalysis, 2018, 358, 199-210.	6.2	80
25	Technetium and iodine aqueous species immobilization and transformations in the presence of strong reductants and calcite-forming solutions: Remedial action implications. Science of the Total Environment, 2018, 636, 588-595.	8.0	17
26	Redox Fluctuations Control the Coupled Cycling of Iron and Carbon in Tropical Forest Soils. Environmental Science & Technology, 2018, 52, 14129-14139.	10.0	96
27	Interactions Between Fe(III)-oxides and Fe(III)-phyllosilicates During Microbial Reduction 2: Natural Subsurface Sediments. Geomicrobiology Journal, 2017, 34, 231-241.	2.0	14
28	Transformation of Active Sites in Fe/SSZ-13 SCR Catalysts during Hydrothermal Aging: A Spectroscopic, Microscopic, and Kinetics Study. ACS Catalysis, 2017, 7, 2458-2470.	11.2	89
29	Tetragonal-Like Phase in Core–Shell Iron Iron-Oxide Nanoclusters. Journal of Physical Chemistry C, 2017, 121, 11794-11803.	3.1	3
30	Solid-Phase Fe Speciation along the Vertical Redox Gradients in Floodplains using XAS and Mössbauer Spectroscopies. Environmental Science & Technology, 2017, 51, 7903-7912.	10.0	58
31	Efficacy of acetate-amended biostimulation for uranium sequestration: Combined analysis of sediment/groundwater geochemistry and bacterial community structure. Applied Geochemistry, 2017, 78, 172-185.	3.0	18
32	Reduced Magnetism in Core–Shell Magnetite@MOF Composites. Nano Letters, 2017, 17, 6968-6973.	9.1	47
33	Mössbauer Spectral Properties of Yttrium Iron Garnet, Y <sub>3</sub> Fe <sub>5</sub> O <sub>12</sub> , and Its Isovalent and Nonisovalent Yttrium-Substituted Solid Solutions. Inorganic Chemistry, 2016, 55, 3413-3418.	4.0	8
34	Iron Loading Effects in Fe/SSZ-13 NH <sub>3</sub> -SCR Catalysts: Nature of the Fe Ions and Structure–Function Relationships. ACS Catalysis, 2016, 6, 2939-2954.	11.2	126
35	Structure and thermodynamics of uranium-containing iron garnets. Geochimica Et Cosmochimica Acta, 2016, 189, 269-281.	3.9	41
36	Fe(II) sorption on pyrophyllite: Effect of structural Fe(III) (impurity) in pyrophyllite on nature of layered double hydroxide (LDH) secondary mineral formation. Chemical Geology, 2016, 439, 152-160.	3.3	28

#	Article	IF	CITATIONS
37	Redoxâ€Active Metal–Organic Composites for Highly Selective Oxygen Separation Applications. Advanced Materials, 2016, 28, 3572-3577.	21.0	55
38	Iron mineralogy and uranium-binding environment in the rhizosphere of a wetland soil. Science of the Total Environment, 2016, 569-570, 53-64.	8.0	21
39	Anomalous water expulsion from carbon-based rods at high humidity. Nature Nanotechnology, 2016, 11, 791-797.	31.5	11
40	Interactions Between Fe(III)-Oxides and Fe(III)-Phyllosilicates During Microbial Reduction 1: Synthetic Sediments. Geomicrobiology Journal, 2016, 33, 793-806.	2.0	7
41	Switchable Ionic Liquids: An Environmentally Friendly Medium to Synthesise Nanoparticulate Green Rust. Current Inorganic Chemistry, 2016, 6, 92-99.	0.2	6
42	Uranium fate in Hanford sediment altered by simulated acid waste solutions. Applied Geochemistry, 2015, 63, 1-9.	3.0	9
43	Organic Matter Remineralization Predominates Phosphorus Cycling in the Mid-Bay Sediments in the Chesapeake Bay. Environmental Science & amp; Technology, 2015, 49, 5887-5896.	10.0	117
44	Biological Redox Cycling of Iron in Nontronite and Its Potential Application in Nitrate Removal. Environmental Science & Technology, 2015, 49, 5493-5501.	10.0	109
45	Charge-Coupled Substituted Garnets (Y <sub>3–<i>x</i></sub> Ca <sub>0.5<i>x</i></sub> M <sub>0.5<i>x</i></sub> )Fe <sub>5</sub> O <sub>12(M = Ce, Th): Structure and Stability as Crystalline Nuclear Waste Forms. Inorganic Chemistry, 2015, 54, 4156-4166.</sub>	ub> 4.0	29
46	<sup>99</sup> Tc(VII) Retardation, Reduction, and Redox Rate Scaling in Naturally Reduced Sediments. Environmental Science & Technology, 2015, 49, 13403-13412.	10.0	15
47	Influence of Coprecipitated Organic Matter on Fe <sup>2+</sup> <sub>(aq)</sub> -Catalyzed Transformation of Ferrihydrite: Implications for Carbon Dynamics. Environmental Science & Technology, 2015, 49, 10927-10936.	10.0	192
48	Nepheline crystallization in boron-rich alumino-silicate glasses as investigated by multi-nuclear NMR, Raman, & Mössbauer spectroscopies. Journal of Non-Crystalline Solids, 2015, 409, 149-165.	3.1	42
49	Fe/SSZ-13 as an NH3-SCR catalyst: A reaction kinetics and FTIR/Mössbauer spectroscopic study. Applied Catalysis B: Environmental, 2015, 164, 407-419.	20.2	108
50	Syntrophic Effects in a Subsurface Clostridial Consortium on Fe(III)-(Oxyhydr)oxide Reduction and Secondary Mineralization. Geomicrobiology Journal, 2014, 31, 101-115.	2.0	13
51	The solubility of 242PuO2 in the presence of aqueous Fe(II): the impact of precipitate preparation. Radiochimica Acta, 2014, 102, 861.	1.2	0
52	Geochemical and mineralogical investigation of uranium in multi-element contaminated, organic-rich subsurface sediment. Applied Geochemistry, 2014, 42, 77-85.	3.0	40
53	Cerium Substitution in Yttrium Iron Garnet: Valence State, Structure, and Energetics. Chemistry of Materials, 2014, 26, 1133-1143.	6.7	53
54	Mobilization of metals from Eau Claire siltstone and the impact of oxygen under geological carbon dioxide sequestration conditions. Geochimica Et Cosmochimica Acta, 2014, 141, 62-82.	3.9	25

#	Article	IF	CITATIONS
55	Oxidative Remobilization of Technetium Sequestered by Sulfide-Transformed Nano Zerovalent Iron. Environmental Science & Technology, 2014, 48, 7409-7417.	10.0	73
56	Reductive Sequestration of Pertechnetate ( <sup>99</sup> TcO <sub>4</sub> <sup>–</sup> ) by Nano Zerovalent Iron (nZVI) Transformed by Abiotic Sulfide. Environmental Science & Technology, 2013, 47, 5302-5310.	10.0	162
5 <b>7</b>	Biological oxidation of Fe(II) in reduced nontronite coupled with nitrate reduction by Pseudogulbenkiania sp. Strain 2002. Geochimica Et Cosmochimica Acta, 2013, 119, 231-247.	3.9	88
58	Abiotic U(VI) reduction by sorbed Fe(II) on natural sediments. Geochimica Et Cosmochimica Acta, 2013, 117, 266-282.	3.9	43
59	Abiotic Reductive Immobilization of U(VI) by Biogenic Mackinawite. Environmental Science & Technology, 2013, 47, 2361-2369.	10.0	100
60	Oxidative dissolution of UO2 in a simulated groundwater containing synthetic nanocrystalline mackinawite. Geochimica Et Cosmochimica Acta, 2013, 102, 175-190.	3.9	61
61	Microbial Lithotrophic Oxidation of Structural Fe(II) in Biotite. Applied and Environmental Microbiology, 2012, 78, 5746-5752.	3.1	94
62	Microbial Reductive Transformation of Phyllosilicate Fe(III) and U(VI) in Fluvial Subsurface Sediments. Environmental Science & Technology, 2012, 46, 3721-3730.	10.0	34
63	Isolation and Microbial Reduction of Fe(III) Phyllosilicates from Subsurface Sediments. Environmental Science & Technology, 2012, 46, 11618-11626.	10.0	21
64	Effects of redox cycling of iron in nontronite on reduction of technetium. Chemical Geology, 2012, 291, 206-216.	3.3	75
65	Synthesis and properties of titanomagnetite (Fe3â^'xTixO4) nanoparticles: A tunable solid-state Fe(II/III) redox system. Journal of Colloid and Interface Science, 2012, 387, 24-38.	9.4	80
66	Iron oxide waste form for stabilizing 99Tc. Journal of Nuclear Materials, 2012, 429, 201-209.	2.7	46
67	Biotic and Abiotic Pathways of Phosphorus Cycling in Minerals and Sediments: Insights from Oxygen Isotope Ratios in Phosphate. Environmental Science & Technology, 2011, 45, 6254-6261.	10.0	66
68	The mineralogic transformation of ferrihydrite induced by heterogeneous reaction with bioreduced anthraquinone disulfonate (AQDS) and the role of phosphate. Geochimica Et Cosmochimica Acta, 2011, 75, 6330-6349.	3.9	33
69	Bioreduction of Fe-bearing clay minerals and their reactivity toward pertechnetate (Tc-99). Geochimica Et Cosmochimica Acta, 2011, 75, 5229-5246.	3.9	128
70	Size effects on gamma radiation response of magnetic properties of barium hexaferrite powders. Journal of Applied Physics, 2011, 110, .	2.5	5
71	Microbial and Mineralogical Characterizations of Soils Collected from the Deep Biosphere of the Former Homestake Gold Mine, South Dakota. Microbial Ecology, 2010, 60, 539-550.	2.8	70
72	Bioavailability of Fe(III) In Loess Sediments: An Important Source of Electron Acceptors. Clays and Clay Minerals, 2010, 58, 542-557.	1.3	10

**Ravi K Kukkadapu** 

#	Article	IF	CITATIONS
73	Fractionation of oxygen isotopes in phosphate during its interactions with iron oxides. Geochimica Et Cosmochimica Acta, 2010, 74, 1309-1319.	3.9	85
74	Microbial reduction of uranium under iron- and sulfate-reducing conditions: Effect of amended goethite on microbial community composition and dynamics. Water Research, 2010, 44, 4015-4028.	11.3	45
75	Biomineralization associated with microbial reduction of Fe3+ and oxidation of Fe2+ in solid minerals. American Mineralogist, 2009, 94, 1049-1058.	1.9	30
76	Reduction of Hg(II) to Hg(0) by Magnetite. Environmental Science & amp; Technology, 2009, 43, 5307-5313.	10.0	138
77	Uranium in Framboidal Pyrite from a Naturally Bioreduced Alluvial Sediment. Environmental Science & Technology, 2009, 43, 8528-8534.	10.0	85
78	Uranium Extraction From Laboratory-Synthesized, Uranium-Doped Hydrous Ferric Oxides. Environmental Science & Technology, 2009, 43, 2341-2347.	10.0	26
79	Reduction of Tc(VII) by Fe(II) Sorbed on Al (hydr)oxides. Environmental Science & Technology, 2008, 42, 5499-5506.	10.0	69
80	Long-term dynamics of uranium reduction/reoxidation under low sulfate conditions. Geochimica Et Cosmochimica Acta, 2008, 72, 3603-3615.	3.9	111
81	Biogeochemical Processes In Ethanol Stimulated Uranium-contaminated Subsurface Sediments. Environmental Science & Technology, 2008, 42, 4384-4390.	10.0	49
82	Biostimulation of iron reduction and subsequent oxidation of sediment containing Fe-silicates and Fe-oxides: Effect of redox cycling on Fe(III) bioreduction. Water Research, 2007, 41, 2996-3004.	11.3	60
83	Reduction of pertechnetate [Tc(VII)] by aqueous Fe(II) and the nature of solid phase redox products. Geochimica Et Cosmochimica Acta, 2007, 71, 2137-2157.	3.9	154
84	Phosphate Imposed Limitations on Biological Reduction and Alteration of Ferrihydrite. Environmental Science & amp; Technology, 2007, 41, 166-172.	10.0	160
85	Reductive biotransformation of Fe in shale–limestone saprolite containing Fe(III) oxides and Fe(II)/Fe(III) phyllosilicates. Geochimica Et Cosmochimica Acta, 2006, 70, 3662-3676.	3.9	67
86	Microbial reduction of fe(III) in the Fithian and Muloorina illites: contrasting extents and rates of bioreduction. Clays and Clay Minerals, 2006, 54, 67-79.	1.3	51
87	Anaerobic redox cycling of iron by freshwater sediment microorganisms. Environmental Microbiology, 2006, 8, 100-113.	3.8	290
88	Effects of sediment iron mineral composition on microbially mediated changes in divalent metal speciation: Importance of ferrihydrite. Geochimica Et Cosmochimica Acta, 2005, 69, 1739-1754.	3.9	41
89	Control of Fe(III) site occupancy on the rate and extent of microbial reduction of Fe(III) in nontronite. Geochimica Et Cosmochimica Acta, 2005, 69, 5429-5440.	3.9	142
90	Ferrous hydroxy carbonate is a stable transformation product of biogenic magnetite. American Mineralogist, 2005, 90, 510-515.	1.9	75

#	Article	IF	CITATIONS
91	Copper Sorption Mechanisms on Smectites. Clays and Clay Minerals, 2004, 52, 321-333.	1.3	78
92	Biogeochemical transformation of Fe minerals in a petroleum-contaminated aquifer. Geochimica Et Cosmochimica Acta, 2004, 68, 1791-1805.	3.9	49
93	Reduction of TcO4â^' by sediment-associated biogenic Fe(II). Geochimica Et Cosmochimica Acta, 2004, 68, 3171-3187.	3.9	184
94	Biotransformation of two-line silica-ferrihydrite by a dissimilatory Fe(III)-reducing bacterium: formation of carbonate green rust in the presence of phosphate. Geochimica Et Cosmochimica Acta, 2004, 68, 2799-2814.	3.9	164
95	Synthesis of Colloidal Mn2+:ZnO Quantum Dots and High-TCFerromagnetic Nanocrystalline Thin Films. Journal of the American Chemical Society, 2004, 126, 9387-9398.	13.7	394
96	Influence of electron donor/acceptor concentrations on hydrous ferric oxide (HFO) bioreduction. Biodegradation, 2003, 14, 91-103.	3.0	69
97	Microbial Reduction of Structural Fe(III) in Illite and Goethite. Environmental Science & Technology, 2003, 37, 1268-1276.	10.0	128
98	Mössbauer and optical spectroscopic study of temperature and redox effects on iron local environments in a Fe-doped (0.5 mol% Fe2O3) 18Na2O–72SiO2 glass. Journal of Non-Crystalline Solids, 2003, 317, 301-318.	3.1	30
99	Secondary mineralization pathways induced by dissimilatory iron reduction of ferrihydrite under advective flow. Geochimica Et Cosmochimica Acta, 2003, 67, 2977-2992.	3.9	561
100	Transformation of 2-line ferrihydrite to 6-line ferrihydrite under oxic and anoxic conditions. American Mineralogist, 2003, 88, 1903-1914.	1.9	114
101	Biomineralization of Poorly Crystalline Fe(III) Oxides by Dissimilatory Metal Reducing Bacteria (DMRB). Geomicrobiology Journal, 2002, 19, 179-207.	2.0	349
102	Dissimilatory bacterial reduction of Al-substituted goethite in subsurface sediments. Geochimica Et Cosmochimica Acta, 2001, 65, 2913-2924.	3.9	98
103	Biotransformation of Ni-Substituted Hydrous Ferric Oxide by an Fe(III)-Reducing Bacterium. Environmental Science & Technology, 2001, 35, 703-712.	10.0	83
104	Kinetics and Mechanism of Birnessite Reduction by Catechol. Soil Science Society of America Journal, 2001, 65, 58-66.	2.2	61
105	A study of the corrosion products of mild steel in high ionic strength brines. Waste Management, 2001, 21, 335-341.	7.4	8
106	Mineral transformations associated with the microbial reduction of magnetite. Chemical Geology, 2000, 169, 299-318.	3.3	180
107	2H Solid-State NMR Investigation of Terephthalate Dynamics and Orientation in Mixed-Anion Hydrotalcite-Like Compounds. Journal of Physical Chemistry B, 1999, 103, 5197-5203.	2.6	16
108	Adsorption of phenol and chlorinated phenols from aqueous solution by tetramethylammonium- and tetramethylphosphonium-exchanged montmorillonite. Applied Clay Science, 1998, 13, 13-20.	5.2	119

#	Article	IF	CITATIONS
109	Synthesis of a Low-Carbonate High-Charge Hydrotalcite-like Compound at Ambient Pressure and Atmosphere. Chemistry of Materials, 1997, 9, 417-419.	6.7	30
110	Tetramethylphosphonium- and Tetramethylammonium-Smectites as Adsorbents of Aromatic and Chlorinated Hydrocarbons: Effect of Water on Adsorption Efficiency. Clays and Clay Minerals, 1995, 43, 318-323.	1.3	84
111	Studies of the oxidation state and location of palladium species in Al13-pillared montmorillonite. Journal of the Chemical Society, Faraday Transactions, 1991, 87, 3083.	1.7	7
112	Electron spin resonance and X-ray diffraction studies of copper(II)-ion-doped Zr4-pillared montmorillonite clay. Journal of the Chemical Society, Faraday Transactions, 1990, 86, 691.	1.7	11
113	Synthesis and electron spin resonance studies of copper-doped alumina-pillared montmorillonite clay. The Journal of Physical Chemistry, 1988, 92, 6073-6078.	2.9	31
114	Stability of mineralâ€organic matter associations under varying biogeochemical conditions. Soil Science Society of America Journal, 0, , .	2.2	0
115	Selective Interactions of Soil Organic Matter Compounds with Calcite and the Role of Aqueous Ca. ACS Earth and Space Chemistry, 0, , .	2.7	4